SC-MAG-650

A Training Mechanism in Superconducting Accelerator Magnets*

Shlomo Caspi and Alan Lietzke

Lawrence Berkeley National Laboratory
University Of California
Berkeley, CA 94720

January 13, 1999

s_caspi@lbl.gov
(510) 486–7244

* This was supported by the Director, Office of Energy Research, Office of High Energy and Nuclear Physics, High Energy Physics Division, U. S. Department of Energy, under Contract No. DE-AC03–76SF098.

Abstract

We describe and discuss a possible "training" mechanism that has been previously overlooked.

We believe that standard accelerator assembly procedures cause portions of NbTi cables to be in axial compression. This axial compression causes partial decabling. Strands displacement is maintained during collaring. Axial Lorentz forces attempt to pull displaced strands back into place and azimuthal Lorentz unloading facilitates stick-slip movement.

A simple 2-D model allows estimates of the stress/strain conditions near the "ends" under various conditions. We apply this model to the inner layer of the Fermi IR quad and suggest possible ways to reduce training.

Although what we propose here applies directly to NbTi magnets wound under tension we expect the tension in Nb_3Sn magnets to be relieved and annealed during the high temperature reaction. The reduced state of axial compression in Nb_3Sn magnets is expected to substantially decrease training in such magnets, caused by this mechanism.

This work was motivated by an attempt to improve LHC IR quadrupole "training".

Prologue

Many accelerator magnets are made from NbTi "Rutherford" cable. The cable can withstand some degree of tension but decables under compression. Wrapping the cable with insulation reduces the amount of decabling but does not eliminate it (the curing process does not prevent strands from slipping either).

Coils are wound under tension — 75 lb are used when the cable is wrapped around the pole key of the Fermi quad. When additional turns are wrapped the accumulated force is reacted by the "nose" on both ends. Layer 1 of the Fermi quad uses 14 turns corresponding to a total force on the "nose" of 2100 lb (75x14x2). As the coil comes out of curing it is under axial tension and the pole key under axial compression (Fig. 1 top). At this point an important and crucial step occurs — the pole key is removed from coil. Where do 2100 lb of tension go once the coil reaches self equilibrium? Suppose we have a long coil and we observe what happens at its center when the pole key is gone. We argue, that the windings there "see" very little of what transpires at the "ends", maintaining most of their axial tension. Things change drastically as we approach the ends. The removal of the "nose" removes the reacting force and moves the conductor into a new equilibrium by reducing the tension in the cable. Due to the accumulated nature of the forces the outer most turns (near the mid plane) move inward less than turns near the pole. Axial equilibrium is reached when the force on about 1/2 the turns near the midplane, still in tension, are balanced by a reaction force produced by the rest of the turns near the pole now under axial compression (Fig. 1 bottom)(in the "end" the arc length of the inner turns is shorter than the outer turns). The degree of compression varies from a maximum near the ends to 0 compression some distance away and low tension in the rest of the body. The size of the region under compression depends on the cable's width, winding force, and type of insulation. We assume its length may be of the order of several bore diameters. It is this region under axial compression that we draw our attention to.

Take a cable and compress it along its length, one can easily observe how the strands tend to separate from each other. With insulation the separation is somewhat inhibited but it's still

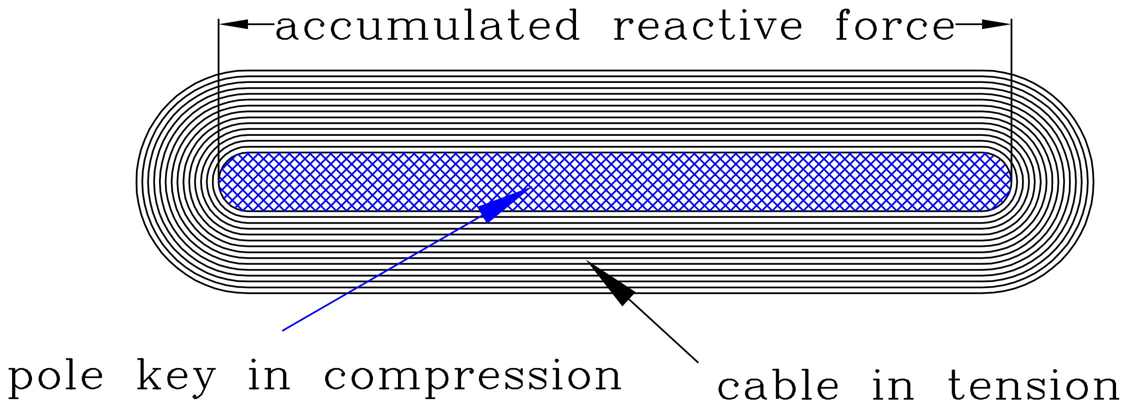

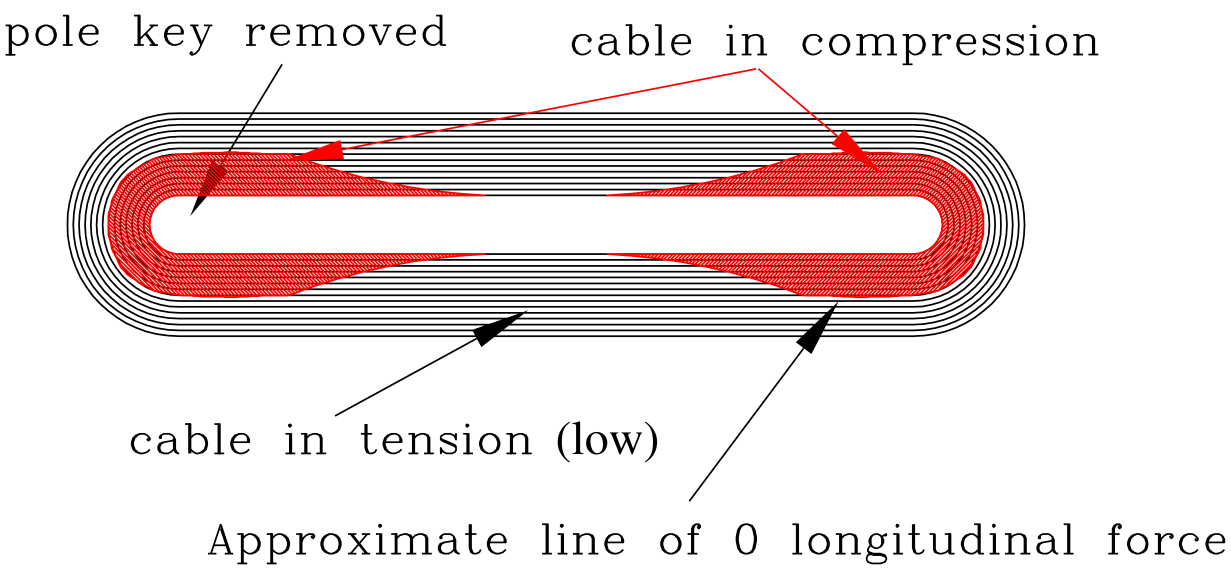

Figure 1 Cured coil with pole key in (top), and with pole key removed (bottom).

there. We point out that epoxy is placed on the side that faces away from the cable, leaving the cable free to slide within. If we try and simulate a stress-strain curve that covers both axial tension and compression, it may look somewhat like the curve in Fig. 2. If the cable is supported on both sides by other cables or wedges its integrity will be maintained to a degree. However cables that have no side support, like the turn next to the pole, may see strand displacements even under low compression.

We assume therefore that the cable integrity in a compressed region may not be preserved, with a high likelihood of decabling along the pole turn due to lack of side support and high axial compression.

When the magnet is collared and placed under azimuthal compression (θ direction) the axially compressed regions are left unaffected.

We point out again that what maintains the cable integrity is the locking mechanisms between strands or the “knuckles”. Under tension strands interlock whereas under compression they

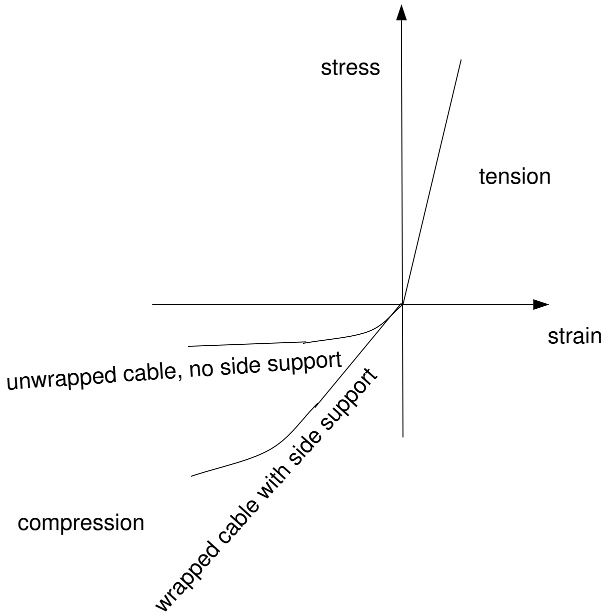

Figure 2 A stress strain curve for a cable under axial tension and compression.

simply move apart (Fig. 3).

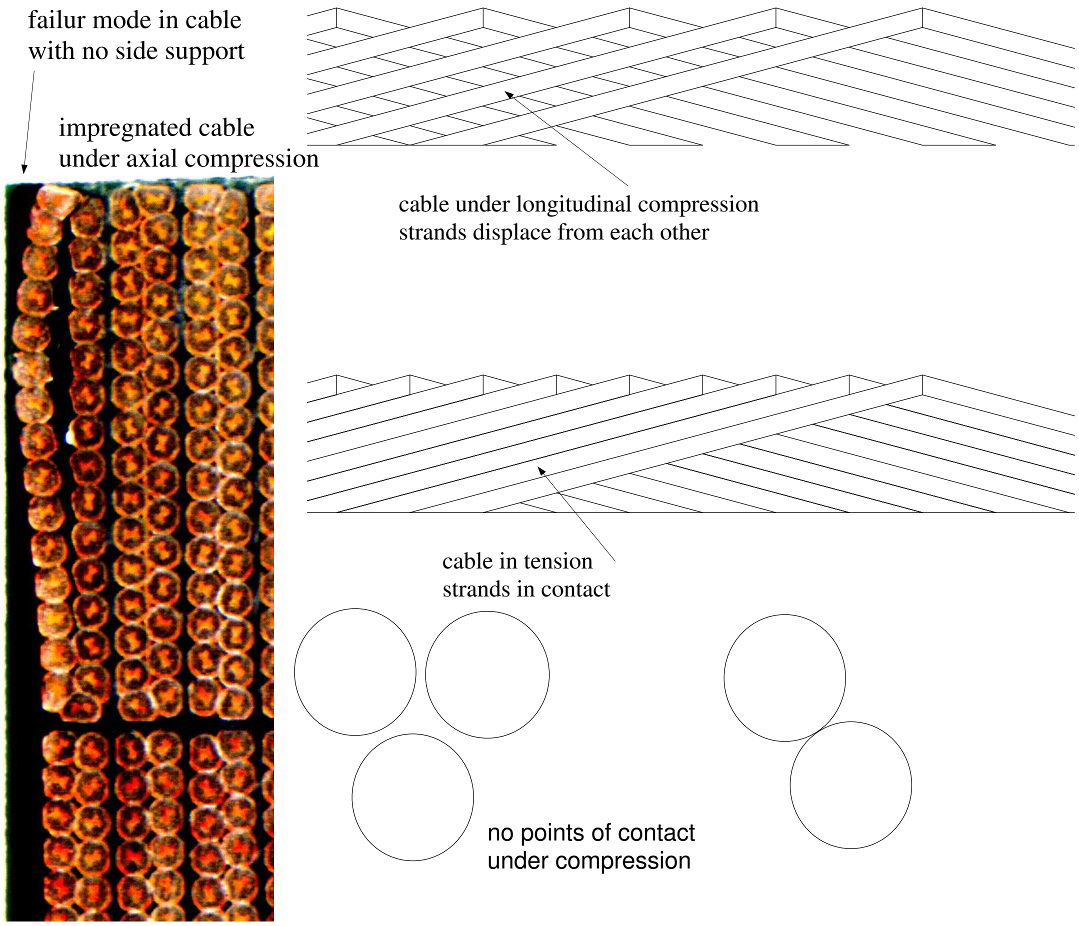

Figure 3 Under tension strands stay together. Under compression and without side support strands tend to separate and decable.

Training

When the magnet is energized, end forces attempt to stretch it even if the magnet is restrained by end plates. Turn to turn strain and motion will occur. When such forces increase, the degree of compression (along the cables) near the ends will diminish and may eventually disappear with the cable going into tension. The process may be enhanced by the fact that while axial forces increase, prestress near the pole and in the θ direction decreases. The combined effect increases the chances of strands within the pole turn to displace axially seeking a new local equilibrium. It is conceivable that while this process occurs strands generate frictional heating that may quench the magnet. Other sources such as a very low azimuthal (θ) prestress also contribute to the training process, however we assume that the magnets are adequately prestressed.

Reduce Training

Based on what has been described magnet performance can improve by eliminating the state of axial compression near the ends. One way to do so is not to remove the pole keys. This however may not be possible when collars are used. We can also consider splitting the collars by making the pole an integral part of the coil never to be removed. The other choice is to STRETCH the magnet back to its original position (and beyond), a process that is not simple but quite possible. We also recommend to wind each coil with the highest possible tension and gradually reduce the tension when each subsequent turn is wrapped on.

Evidence

So far longitudinal compression in cables was given little attention. We list some of the limited evidence we have on that:

1. When LBL built its 17 m long SSC dipoles at BNL, it maintained constant winding tension in the coil windings. After the magnets were cured and the pole key removed the inner turns in the end region developed many turn to turn shorts.
2. Tests on long SSC magnets proved that training is not length dependent and is much more a “localized” phenomenon.
3. In the early 90’s LBNL has built a 1 m long SSC dipole (D19) with thin elliptical collars. This magnet reached it short sample limit on its first quench (central field of 7.6 T). This coil was stretched to its original axial position. At 1.8 K the magnet reached 10 T after a series of training quenches suggesting that additonal axial streching needs to be considered.

Analysis

We have computed the stress in the windings near the ends of the Fermi LHC quad, assuming:

1. The coil is flat (as shown in Fig. 4) and is plain stress
2. The ends are circular (no straight section)
3. The windings and field are solenoid like.
4. Cable tension and temperature dependence included.
5. Azimuthal or tangential is along the cable direction. Radial refers to the direction across turns or turn to turn.
6. Turns allowed to slide (not “glued”)

Computations were based on the report *“Stress-Strain in Shells Under Mechanical, Thermal, and Magnetic Loads” S. Caspi et al, SC-MAG-616, March 1998. (postscript http://supercon.lbl.gov/caspi/publication/stress_in_shells.ps)*

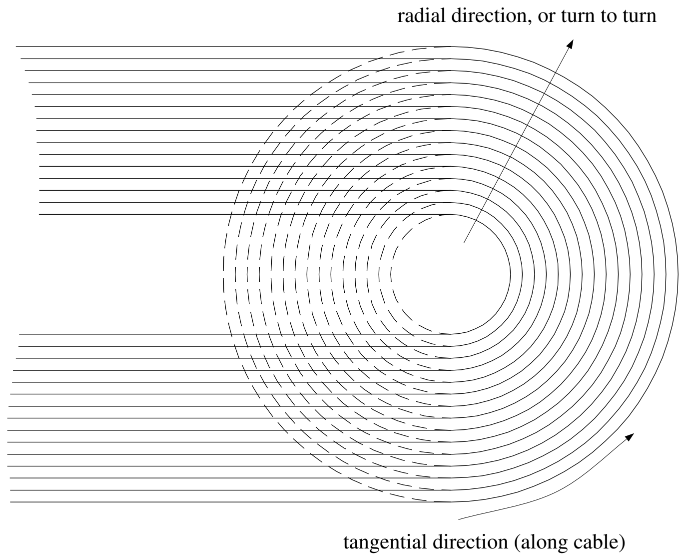

Figure 4 Simulation of accelerator “end” coils as a solenoid.

The cable and the cross section geometry are that of the inner layer of the Fermi LHC IR Quad (Fig. 5).

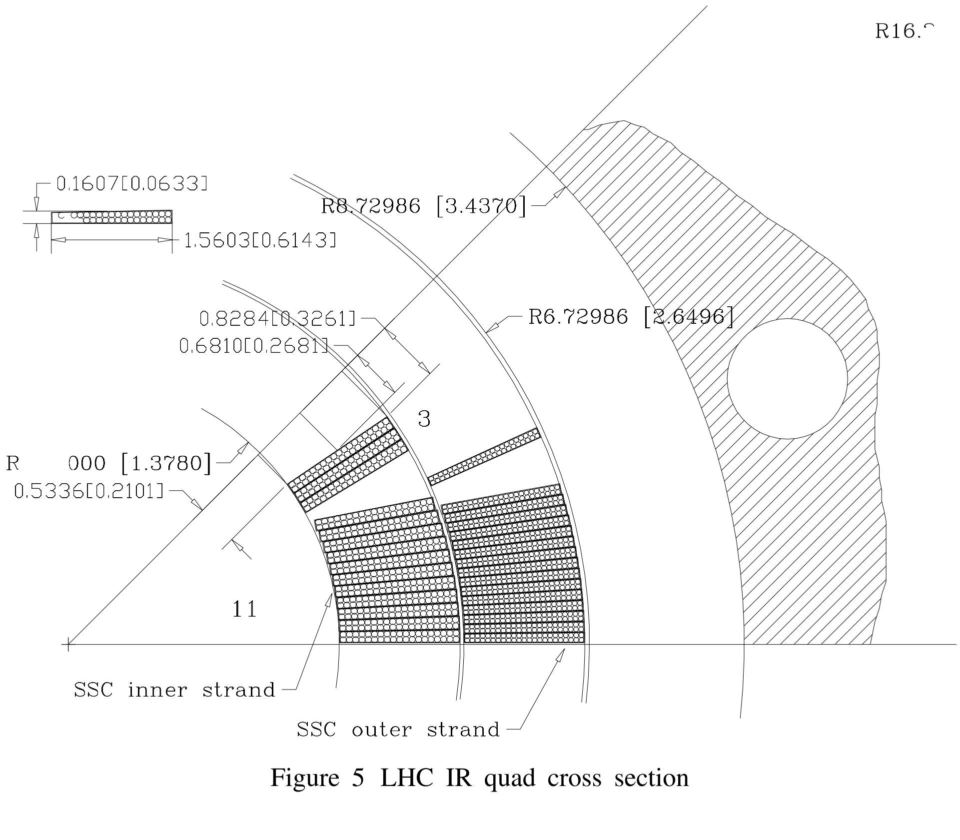

Figure 5 LHC IR quad cross section

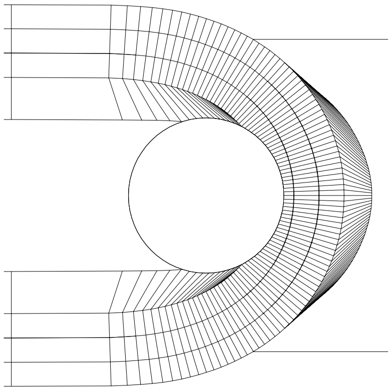

Figure 6 LHC IR quad — top view of "end" region.

As each turn is wrapped with 75 lb of tension inner turns lose some of their tension. When the last turn (14) is wrapped, it is under 14 MPa of tension while the inner turn (1) has reduced it tension to an average 4 MPa. The pole key is now compressed to —27 MPa (Fig. 7 top). Removing the pole key (Fig. 7 bottom), does not change the tension in the outer turn, however all other turns reduce their tension and the inner most 6 turns go into tangential compression, reaching —20 MPa in the inner most turn. Reducing the temperature readjusts the stress distribution. The outer most turn is now at 10 MPa of tension and the inner turn drops to —29 MPa of compression. Figures 8 and 9 show the corresponding radial stress and displacements.

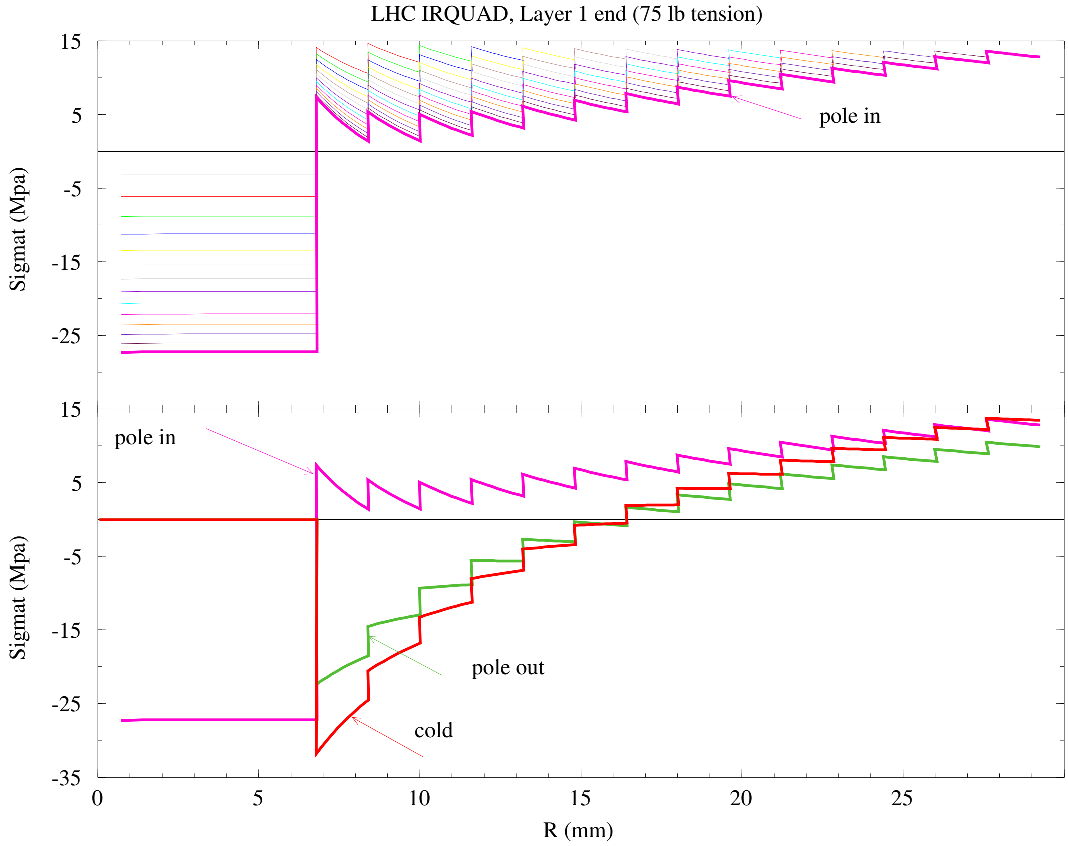

Figure 7 Azimuthal stress, along cable, with pole key in,
equilibrium after pole key has been removed and cool down.

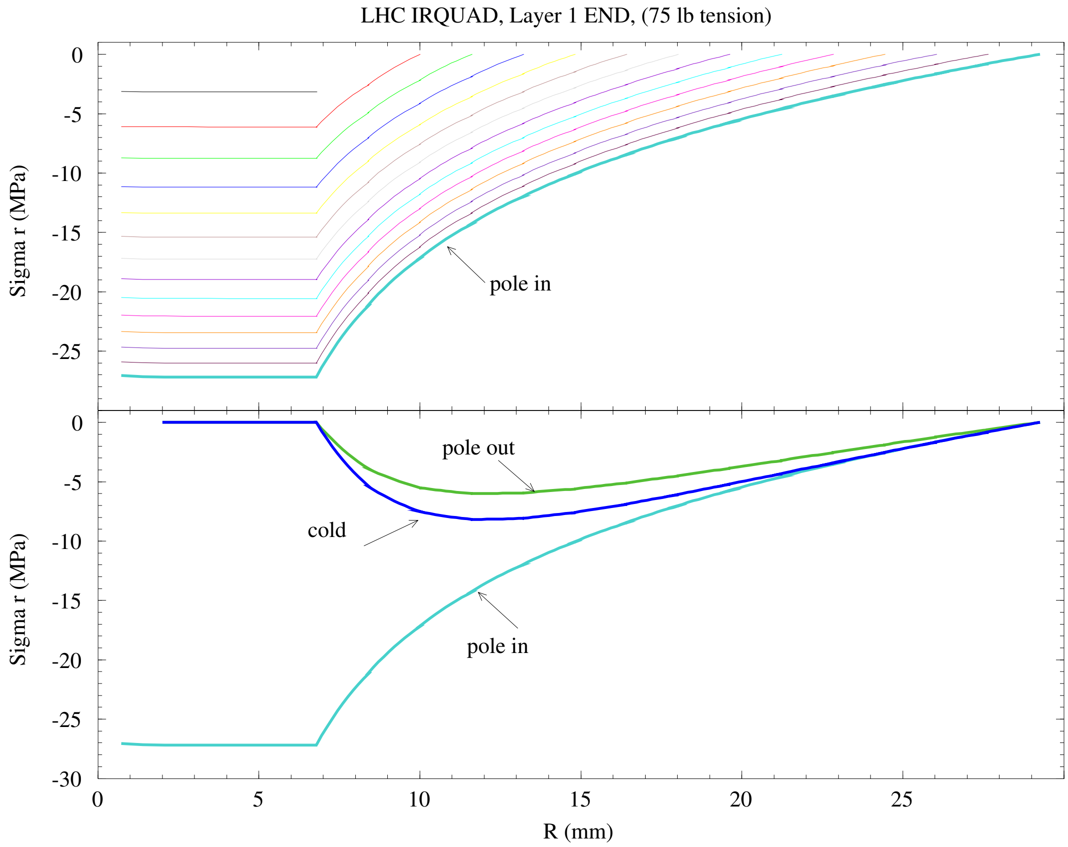

Figure 8 Turn to turn stress (across turns).

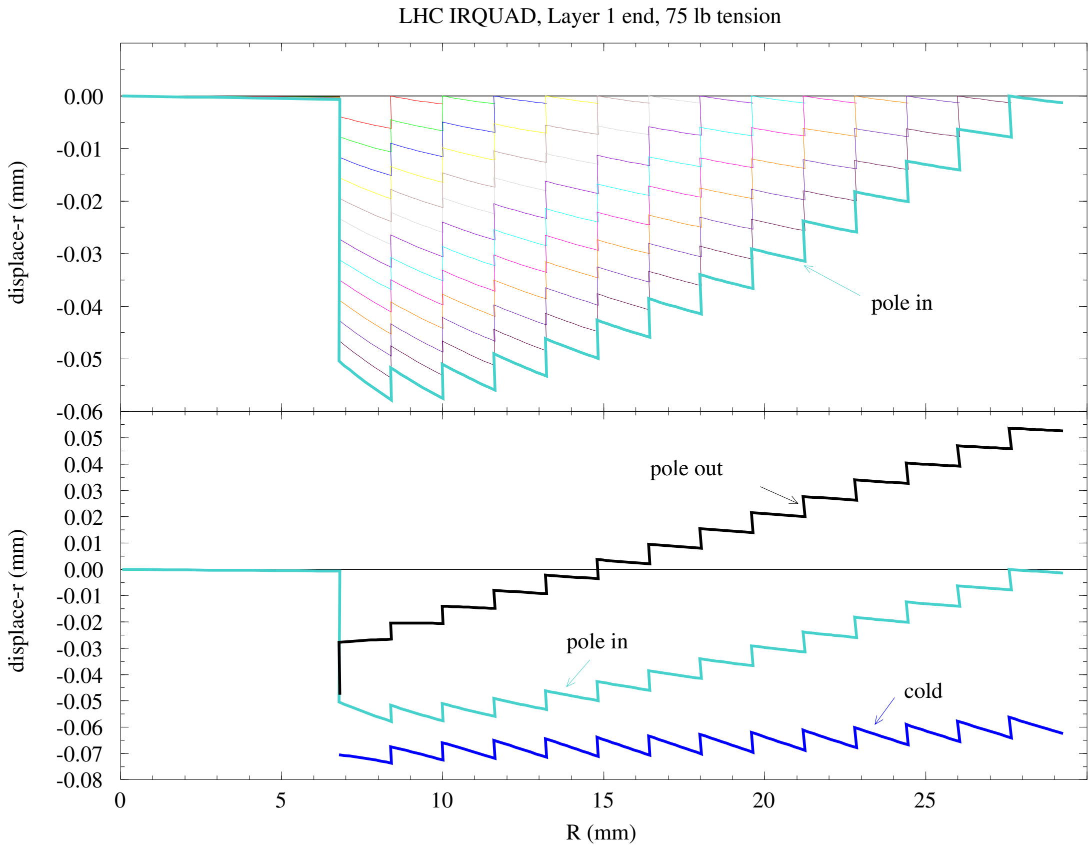

Figure 9 Displacements across turns.

If we now turn on the field (assuming it is solenoidal) and introduce field and currents values that are typical to that of a first quench and the short sample, the stress distribution will be modified to that shown in Figures 10,11 and 12. During the first quench all turns are at 22 MPa of tension, however at short sample the outer turn reaches 35 MPa and the inner turn 65 MPa. In addition, as shown in Fig. 11, the stress across turns (turn to turn) is not fully compressive, 6 turns near the “nose” are now in tension.

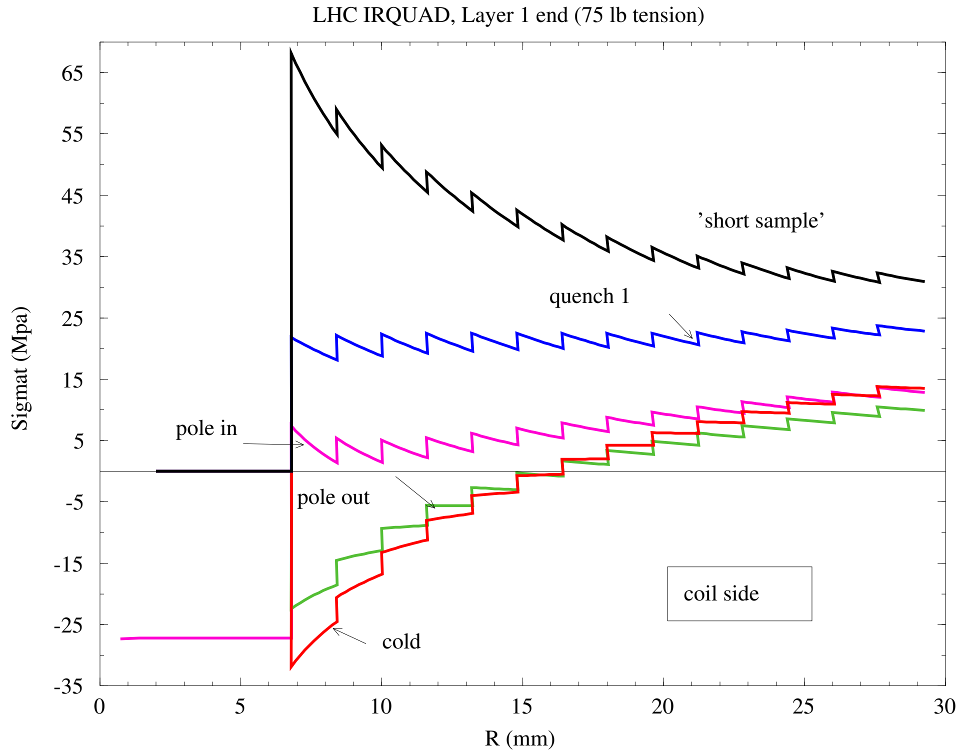

Figure 10 Stress along turns including magnetic forces during quench #1, and short sample field.

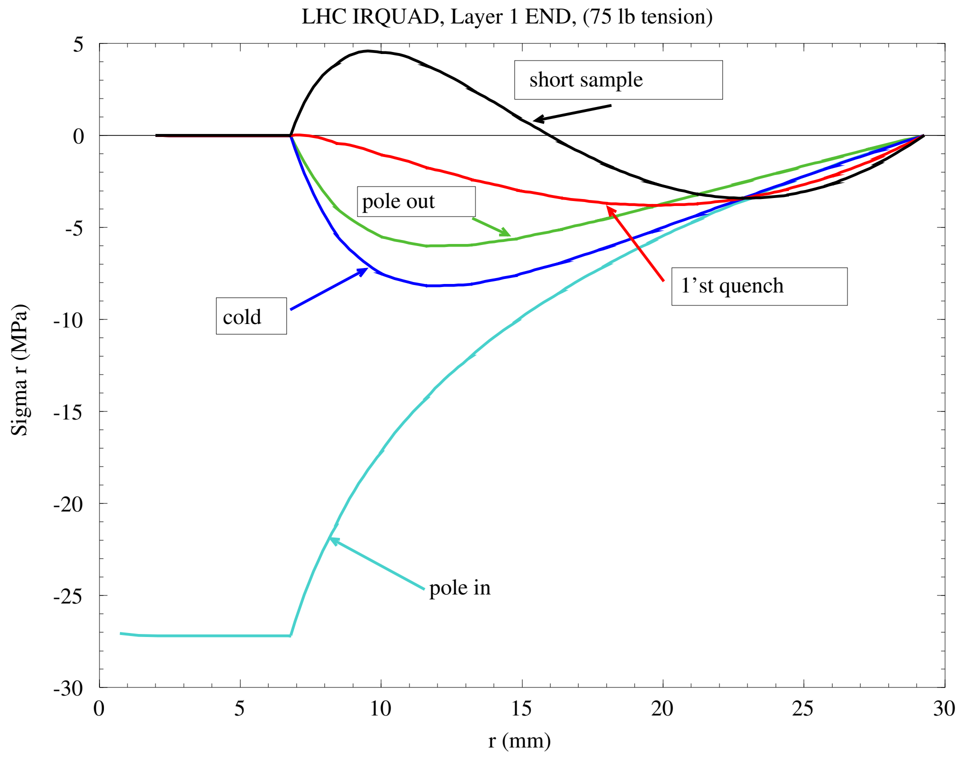

Figure 11 Turn to turn pressure including magnetic forces.

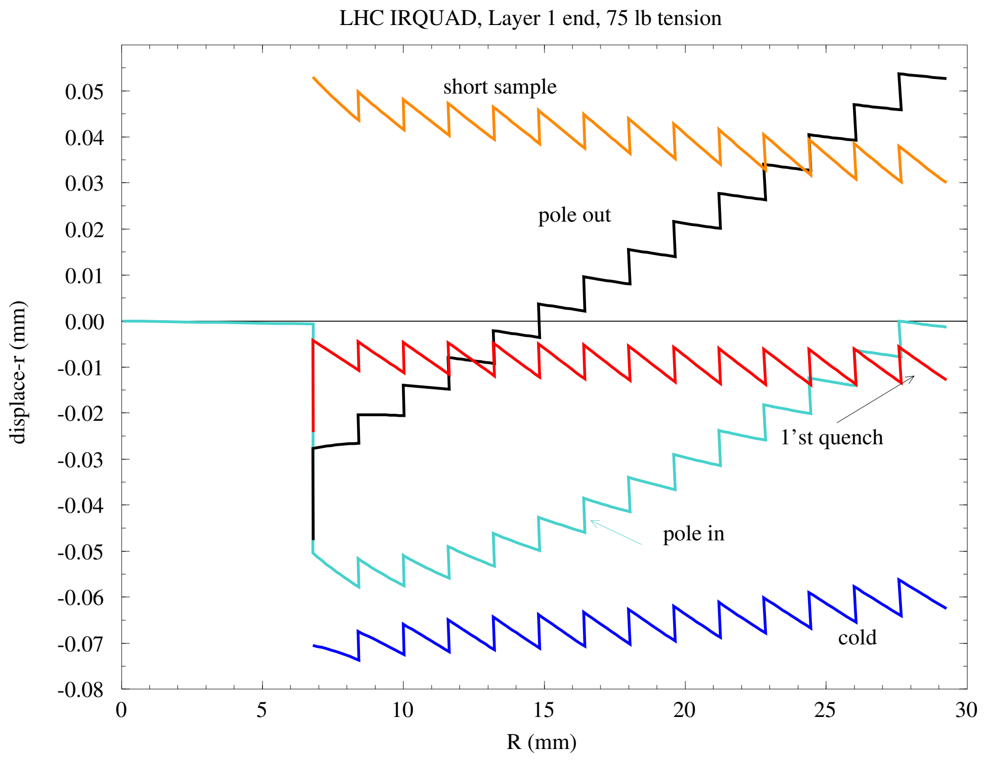

Figure 12 Displacements

If we wish to readjust the force level in the “end” to match the level that corresponds to the initial tension, first quench and final short sample, we shall have to apply on each end a corresponding axial force of 1350 lb, 1975 lb and 3950 lb (Fig. 13).

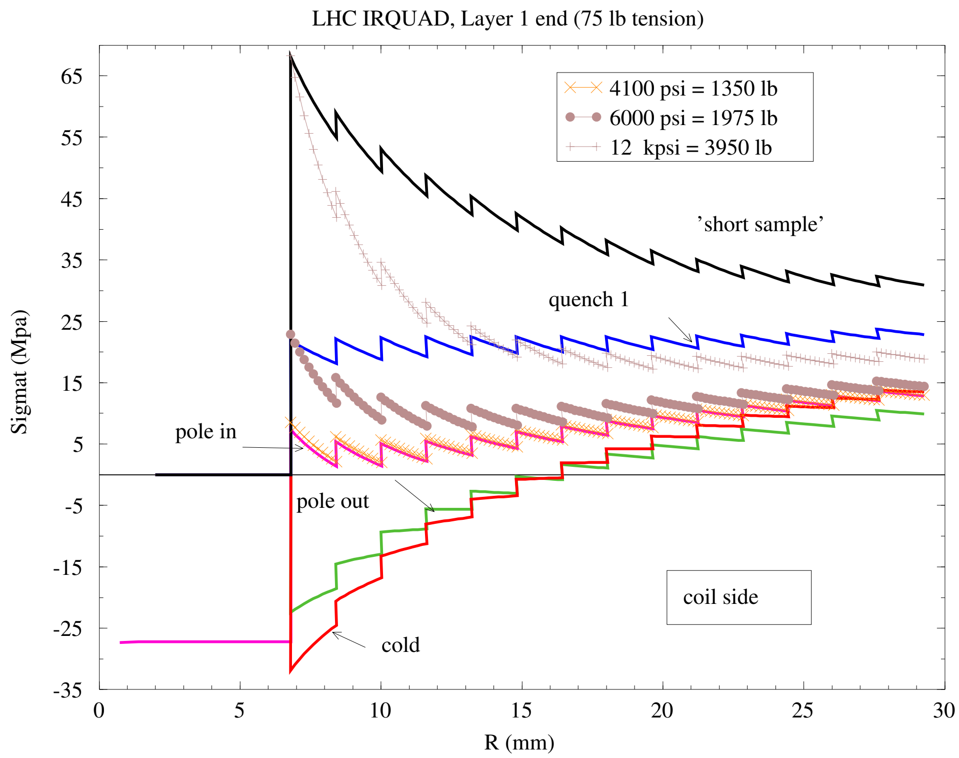

Figure 13 Pressurizing the pole key area to achieve an equivalent cable tension as with Lorentz forces.

Appendix A Input into "Shell"

```
layer  ,Ri ,Ro ,Er ,Et ,Pt alfar,alfat ,Ba        ,Bb  ,current-density, tension (lb/inch)
Interferance
line 3
line 4
0.0D+00  0.0D+00
1  0.05D+00   6.810D+00  1.950D+11 1.950D+11 2.94D-01 0.0D+00  0.0D+00  0.00D+00  0.00D+00  0.0D+00  0.00D+00
0.0d0
14 6.810D+00 2.9308D+01 5.50D+09  5.50D+09 3.0D-01 0.0D+00  0.0D+00  7.25D+00 0.0D+00  0.0D+00  1.22D+02
```

file ***Rt.in***

```
layer  ,Ri ,Ro ,Er ,Et ,Pt alfar,alfat ,Ba        ,Bb  ,current-density, tension (N/m)
Interferance
line 3
line 4
0.0D+00  0.0D+00
  1  5.00D-02  6.810D+00  1.950D+05  1.950D+05 1.00D-03  0.00D+00  0.00D+00  0.00D+00  0.00D+00  0.00D+00  0.00D+00
  1.986968D-02
  2  6.79021D+00  8.41542D+00  5.50D+09  5.50D+09  3.00D-01  0.00D+00  0.00D+00  7.25638D+00  6.73265D+00  0.00D+00  2.13655D+04
  6.170889D-03
  3  8.39106D+00  1.00201D+01  5.50D+09  5.50D+09  3.00D-01  0.00D+00  0.00D+00  6.74050D+00  6.21553D+00  0.00D+00  2.13655D+04
  6.599319D-03
  4  9.99149D+00  1.16244D+01  5.50D+09  5.50D+09  3.00D-01  0.00D+00  0.00D+00  6.22476D+00  5.69854D+00  0.00D+00  2.13655D+04
  6.900375D-03
  5  1.15916D+01  1.32284D+01  5.50D+09  5.50D+09  3.00D-01  0.00D+00  0.00D+00  5.70912D+00  5.18165D+00  0.00D+00  2.13655D+04
  7.117708D-03
  6  1.31916D+01  1.48322D+01  5.50D+09  5.50D+09  3.00D-01  0.00D+00  0.00D+00  5.19354D+00  4.66482D+00  0.00D+00  2.13655D+04
  7.279021D-03
  7  1.47913D+01  1.64359D+01  5.50D+09  5.50D+09  3.00D-01  0.00D+00  0.00D+00  4.67800D+00  4.14805D+00  0.00D+00  2.13655D+04
  7.402012D-03
  8  1.63910D+01  1.80394D+01  5.50D+09  5.50D+09  3.00D-01  0.00D+00  0.00D+00  4.16251D+00  3.63131D+00  0.00D+00  2.13655D+04
  7.498172D-03
  9  1.79906D+01  1.96429D+01  5.50D+09  5.50D+09  3.00D-01  0.00D+00  0.00D+00  3.64704D+00  3.11460D+00  0.00D+00  2.13655D+04
  7.575128D-03
 10  1.95901D+01  2.12462D+01  5.50D+09  5.50D+09  3.00D-01  0.00D+00  0.00D+00  3.13160D+00  2.59791D+00  0.00D+00  2.13655D+04
  7.638052D-03
 11  2.11896D+01  2.28496D+01  5.50D+09  5.50D+09  3.00D-01  0.00D+00  0.00D+00  2.61617D+00  2.08123D+00  0.00D+00  2.13655D+04
  7.690530D-03
 12  2.27890D+01  2.44529D+01  5.50D+09  5.50D+09  3.00D-01  0.00D+00  0.00D+00  2.10075D+00  1.56458D+00  0.00D+00  2.13655D+04
  7.735101D-03
 13  2.43884D+01  2.60561D+01  5.50D+09  5.50D+09  3.00D-01  0.00D+00  0.00D+00  1.58535D+00  1.04793D+00  0.00D+00  2.13655D+04
  7.773594D-03
 14  2.59878D+01  2.76593D+01  5.50D+09  5.50D+09  3.00D-01  0.00D+00  0.00D+00  1.06995D+00  5.31289D-01  0.00D+00  2.13655D+04
  7.807351D-03
 15  2.75871D+01  2.92625D+01  5.50D+09  5.50D+09  3.00D-01  0.00D+00  0.00D+00  5.54564D-01  1.46579D-02  0.00D+00  2.13655D+04
```

file ***nobore.in***

```
layer  ,Ri ,Ro ,Er ,Et ,Pt alfar,alfat ,Ba        ,Bb  ,current-density, tension (N/m)
Interferance
line 3
line 4
0.0D+00  0.0D+00
  1  5.00D-02  6.810D+00  1.950D+05  1.950D+05 1.00D-03  0.00D+00  0.00D+00  0.00D+00  0.00D+00  0.00D+00  0.00D+00
  1.986968D-02
  2  6.79021D+00  8.41542D+00  5.50D+09  5.50D+09  3.0D-01 -0.0029D+00 -0.00459D+00  7.25638D+00  6.73265D+00  0.00D+00  2.13655D+04
  6.170889D-03
  3  8.39106D+00  1.00201D+01  5.50D+09  5.50D+09  3.0D-01 -0.0029D+00 -0.00459D+00  6.74050D+00  6.21553D+00  0.00D+00  2.13655D+04
  6.599319D-03
  4  9.99149D+00  1.16244D+01  5.50D+09  5.50D+09  3.0D-01 -0.0029D+00 -0.00459D+00  6.22476D+00  5.69854D+00  0.00D+00  2.13655D+04
  6.900375D-03
  5  1.15916D+01  1.32284D+01  5.50D+09  5.50D+09  3.0D-01 -0.0029D+00 -0.00459D+00  5.70912D+00  5.18165D+00  0.00D+00  2.13655D+04
  7.117708D-03
  6  1.31916D+01  1.48322D+01  5.50D+09  5.50D+09  3.0D-01 -0.0029D+00 -0.00459D+00  5.19354D+00  4.66482D+00  0.00D+00  2.13655D+04
  7.279021D-03
  7  1.47913D+01  1.64359D+01  5.50D+09  5.50D+09  3.0D-01 -0.0029D+00 -0.00459D+00  4.67800D+00  4.14805D+00  0.00D+00  2.13655D+04
  7.402012D-03
  8  1.63910D+01  1.80394D+01  5.50D+09  5.50D+09  3.0D-01 -0.0029D+00 -0.00459D+00  4.16251D+00  3.63131D+00  0.00D+00  2.13655D+04
  7.498172D-03
  9  1.79906D+01  1.96429D+01  5.50D+09  5.50D+09  3.0D-01 -0.0029D+00 -0.00459D+00  3.64704D+00  3.11460D+00  0.00D+00  2.13655D+04
  7.575128D-03
 10  1.95901D+01  2.12462D+01  5.50D+09  5.50D+09  3.0D-01 -0.0029D+00 -0.00459D+00  3.13160D+00  2.59791D+00  0.00D+00  2.13655D+04
  7.638052D-03
 11  2.11896D+01  2.28496D+01  5.50D+09  5.50D+09  3.0D-01 -0.0029D+00 -0.00459D+00  2.61617D+00  2.08123D+00  0.00D+00  2.13655D+04
  7.690530D-03
 12  2.27890D+01  2.44529D+01  5.50D+09  5.50D+09  3.0D-01 -0.0029D+00 -0.00459D+00  2.10075D+00  1.56458D+00  0.00D+00  2.13655D+04
  7.735101D-03
 13  2.43884D+01  2.60561D+01  5.50D+09  5.50D+09  3.0D-01 -0.0029D+00 -0.00459D+00  1.58535D+00  1.04793D+00  0.00D+00  2.13655D+04
  7.773594D-03
 14  2.59878D+01  2.76593D+01  5.50D+09  5.50D+09  3.0D-01 -0.0029D+00 -0.00459D+00  1.06995D+00  5.31289D-01  0.00D+00  2.13655D+04
  7.807351D-03
 15  2.75871D+01  2.92625D+01  5.50D+09  5.50D+09  3.0D-01 -0.0029D+00 -0.00459D+00  5.54564D-01  1.46579D-02  0.00D+00  2.13655D+04
```

file ***cold.in***

```
layer  ,Ri ,Ro ,Er ,Et ,Pt alfar,alfat ,Ba        ,Bb  ,current-density, tension (N/m)
Interferance
line 3
line 4
0.0D+00  0.0D+00
  1  5.00D-02  6.810D+00  1.950D+05  1.950D+05 1.00D-03  0.00D+00  0.00D+00  0.00D+00  0.00D+00  0.00D+00  0.00D+00
  1.986968D-02
  2  6.79021D+00  8.41542D+00  5.50D+09  5.50D+09  3.0D-01 -0.0029D+00 -0.00459D+00  7.25638D+00  6.73265D+00  415.0d0  2.13655D+04
  6.170889D-03
  3  8.39106D+00  1.00201D+01  5.50D+09  5.50D+09  3.0D-01 -0.0029D+00 -0.00459D+00  6.74050D+00  6.21553D+00  415.0d0  2.13655D+04
  6.599319D-03
  4  9.99149D+00  1.16244D+01  5.50D+09  5.50D+09  3.0D-01 -0.0029D+00 -0.00459D+00  6.22476D+00  5.69854D+00  415.0d0  2.13655D+04
  6.900375D-03
  5  1.15916D+01  1.32284D+01  5.50D+09  5.50D+09  3.0D-01 -0.0029D+00 -0.00459D+00  5.70912D+00  5.18165D+00  415.0d0  2.13655D+04
  7.117708D-03
  6  1.31916D+01  1.48322D+01  5.50D+09  5.50D+09  3.0D-01 -0.0029D+00 -0.00459D+00  5.19354D+00  4.66482D+00  415.0d0  2.13655D+04
  7.279021D-03
  7  1.47913D+01  1.64359D+01  5.50D+09  5.50D+09  3.0D-01 -0.0029D+00 -0.00459D+00  4.67800D+00  4.14805D+00  415.0d0  2.13655D+04
  7.402012D-03
  8  1.63910D+01  1.80394D+01  5.50D+09  5.50D+09  3.0D-01 -0.0029D+00 -0.00459D+00  4.16251D+00  3.63131D+00  415.0d0  2.13655D+04
  7.498172D-03
  9  1.79906D+01  1.96429D+01  5.50D+09  5.50D+09  3.0D-01 -0.0029D+00 -0.00459D+00  3.64704D+00  3.11460D+00  415.0d0  2.13655D+04
  7.575128D-03
 10  1.95901D+01  2.12462D+01  5.50D+09  5.50D+09  3.0D-01 -0.0029D+00 -0.00459D+00  3.13160D+00  2.59791D+00  415.0d0  2.13655D+04
  7.638052D-03
 11  2.11896D+01  2.28496D+01  5.50D+09  5.50D+09  3.0D-01 -0.0029D+00 -0.00459D+00  2.61617D+00  2.08123D+00  415.0d0  2.13655D+04
  7.690530D-03
 12  2.27890D+01  2.44529D+01  5.50D+09  5.50D+09  3.0D-01 -0.0029D+00 -0.00459D+00  2.10075D+00  1.56458D+00  415.0d0  2.13655D+04
  7.735101D-03
 13  2.43884D+01  2.60561D+01  5.50D+09  5.50D+09  3.0D-01 -0.0029D+00 -0.00459D+00  1.58535D+00  1.04793D+00  415.0d0  2.13655D+04
  7.773594D-03
 14  2.59878D+01  2.76593D+01  5.50D+09  5.50D+09  3.0D-01 -0.0029D+00 -0.00459D+00  1.06995D+00  5.31289D-01  415.0d0  2.13655D+04
  7.807351D-03
 15  2.75871D+01  2.92625D+01  5.50D+09  5.50D+09  3.0D-01 -0.0029D+00 -0.00459D+00  5.54564D-01  1.46579D-02  415.0d0  2.13655D+04
```

file ***fieldQ1.in***

```
layer  ,Ri ,Ro ,Er ,Et ,Pt alfar,alfat ,Ba        ,Bb  ,current-density, tension (N/m)
Interferance
line 3
line 4
0.0D+00  0.0D+00
  1  5.00D-02  6.810D+00  1.950D+05  1.950D+05 1.00D-03  0.0D+00  0.00D+00  0.00D+00  0.00D+00  0.00D+00  0.00D+00
  1.986968D-02
  2  6.79021D+00  8.41542D+00  5.50D+09  5.50D+09  3.0D-01 -0.0029D+00 -0.00459D+00  9.90871D+00  9.19355D+00  566.0d0  2.13655D+04
  6.170889D-03
  3  8.39106D+00  1.00201D+01  5.50D+09  5.50D+09  3.0D-01 -0.0029D+00 -0.00459D+00  9.20427D+00  8.48741D+00  566.0d0  2.13655D+04
  6.599319D-03
  4  9.99149D+00  1.16244D+01  5.50D+09  5.50D+09  3.0D-01 -0.0029D+00 -0.00459D+00  8.502D+00  7.78146D+00  566.0d0  2.13655D+04
  6.900375D-03
  5  1.15916D+01  1.32284D+01  5.50D+09  5.50D+09  3.0D-01 -0.0029D+00 -0.00459D+00  7.79590D+00  7.07563D+00  566.0d0  2.13655D+04
  7.117708D-03
  6  1.31916D+01  1.48322D+01  5.50D+09  5.50D+09  3.0D-01 -0.0029D+00 -0.00459D+00  7.09186D+00  6.36990D+00  566.0d0  2.13655D+04
  7.279021D-03
  7  1.47913D+01  1.64359D+01  5.50D+09  5.50D+09  3.0D-01 -0.0029D+00 -0.00459D+00  6.38790D+00  5.66423D+00  566.0d0  2.13655D+04
  7.402012D-03
  8  1.63910D+01  1.80394D+01  5.50D+09  5.50D+09  3.0D-01 -0.0029D+00 -0.00459D+00  5.68398D+00  4.95861D+00  566.0d0  2.13655D+04
  7.498172D-03
  9  1.79906D+01  1.96429D+01  5.50D+09  5.50D+09  3.0D-01 -0.0029D+00 -0.00459D+00  4.98010D+00  4.25304D+00  566.0d0  2.13655D+04
  7.575128D-03
 10  1.95901D+01  2.12462D+01  5.50D+09  5.50D+09  3.0D-01 -0.0029D+00 -0.00459D+00  4.27625D+00  3.54749D+00  566.0d0  2.13655D+04
  7.638052D-03
 11  2.11896D+01  2.28496D+01  5.50D+09  5.50D+09  3.0D-01 -0.0029D+00 -0.00459D+00  3.57242D+00  2.84196D+00  566.0d0  2.13655D+04
  7.690530D-03
 12  2.27890D+01  2.44529D+01  5.50D+09  5.50D+09  3.0D-01 -0.0029D+00 -0.00459D+00  2.86861D+00  2.13645D+00  566.0d0  2.13655D+04
  7.735101D-03
 13  2.43884D+01  2.60561D+01  5.50D+09  5.50D+09  3.0D-01 -0.0029D+00 -0.00459D+00  2.16482D+00  1.43096D+00  566.0d0  2.13655D+04
  7.773594D-03
 14  2.59878D+01  2.76593D+01  5.50D+09  5.50D+09  3.0D-01 -0.0029D+00 -0.00459D+00  1.46104D+00  7.25484D-01  566.0d0  2.13655D+04
  7.807351D-03
 15  2.75871D+01  2.92625D+01  5.50D+09  5.50D+09  3.0D-01 -0.0029D+00 -0.00459D+00  7.57267D-01  2.00156D-02  566.0d0  2.13655D+04
```

file ***fieldQss.in***